ASTRONOMY & ASTROPHYSICS
SUPPLEMENT SERIES

JUNE 1985, PAGE 373

Astron. Astrophys. Suppl. Ser. **60**, 373-388 (1985)

The ultraviolet spectrum of the Be star HD 50138 (*)

D. Hutsemékers (**)

Institut d'Astrophysique, Université de Liège, 5, avenue de Cointe, B-4200 Cointe-Ougrée, Belgium

Received March 10, 1983, accepted January 31, 1985

Summary. — The ultraviolet spectrum of the B8 Ve star HD 50138, recorded during the Dec. 1978-Jan. 1982 period with IUE, is analysed in the present paper. The spectrum is found to be crowded by absorption lines, mostly those of singly ionized iron peak elements. In addition there are broad lines essentially due to superionized species (Si IV, C IV) and a P Cygni profile for the Mg II doublet, similar to that seen in the star AB Aur. A few Fe II emission lines are also detected. The slowly expanding envelope surrounding HD 50138 appears to be decelerated outward with a decreasing ionization. The physical state of this envelope seems to suffer strong variations : a double structure was detected for some of the absorption lines in 1978-79, and is interpreted as due to an outburst. A net increase of the excitation in 1980 is also observed and vanishes in 1982. In order to explain the unusual profiles of the Mg II lines, we discuss a possible fluorescence mechanism driven by Lyβ. An accurate list of line identifications is also provided.

Key words : Be stars — ultraviolet spectra — stellar winds — Fe II lines — line identification.

1. Introduction.

The emission of hydrogen in the spectrum of the bright ($m_v = 6.7$) Be star HD 50138 ([1]) was first observed by Humason in 1921. While this star, with a low $v \sin i$ of 150 km/s (Houziaux, 1960) shows the typical V/R variations common to Be stars, it also displays some peculiarities in the visual spectral range : bright emission of [O I] $\lambda\lambda$6300-6363 and of Fe II lines (episodically [Fe II]) (Struve and Swings, 1940), intense red or violet satellite absorptions of the Balmer lines (Merrill, 1952 ; and Doazan, 1965). A detailed study of radial velocities by Doazan (1965) shows that HD 50138 is surrounded by an expanding envelope with a period of variation of about 50 days. A mass-loss rate of $6.2 \times 10^{-4}\ M_\odot\ \mathrm{yr}^{-1}$ was determined by Kuan and Kuhi (1975).

In the infrared, Allen (1973) reported an excess of radiation while Andrillat and Houziaux (1972) detected strong emission-absorption variations in the O I λ7772 triplet and a very stable emission of O I λ8446.

Combining their data with the ultraviolet observations provided by the S2/68 orbiting telescope, Houziaux and Andrillat (1976) proposed for HD 50138 a model including a B8 V central star surrounded by an H II shell significantly contributing to the continuous emission.

In an analysis, based on IUE spectra, of circumstellar dust around hot stars, Sitko *et al.* (1981) detected C IV in the spectrum of HD 50138 as well as a strong variability in some Fe II line profiles. They noticed the great similarity with AB Aur, an Herbig Ae star.

In this paper we present the data obtained with the International Ultraviolet Explorer satellite (IUE) at the Villafranca Satellite Tracking Station of the European Space Agency (VILSPA) and at the Goddard Space Flight Center (GSFC). The high resolution spectra (SWP 4557 and LWR 3967) were obtained by A. Heck at the request of L. Houziaux, in March 1979. Since many more spectra of HD 50138 had been taken with IUE, the other high resolution images, both SWP and LWR, have been obtained from the IUE archives.

We give a detailed ultraviolet spectral line identification and describe the several types of profiles, their radial velocities and their variations. The observations are interpreted in a tentative empirical model which confirms and extends the model derived from the visual observations.

2. Observations.

Table I summarizes the log of the high resolution ($\lambda\lambda$1150-3200 Å) IUE observations of HD 50138, obtained during the period 1978-1982. The images have been reduced at VILSPA and at GSFC with the standard calibration

(*) Based on observations by the International Ultraviolet Explorer (IUE) collected at the Villafranca Satellite Tracking Station (VILSPA) or dearchived from the Villafranca Data Archive.

(**) Aspirant au Fonds National de la Recherche Scientifique (Belgium).

([1]) MWC 158, BD − 6°1755 ; $\alpha_{1950} = 6^h49^m.0$, $\delta_{1950} = -6°54'$.

procedure. The majority of the images are of good quality. Tables II and III give the list of absorption lines observed in the spectrum of HD 50138 (respectively in SWP 4557 and LWR 3967, obtained in March 1979). The successive columns in the tables give :

1. The observed wavelength in Å, measured on the original plots (λ air if $\lambda > 2000$ Å).
2. The laboratory wavelength.
3. The identification of the principal ions contributing to the line. The different contributions are listed by increasing wavelength.
4. The multiplet number (Moore, 1968), UV below 3100 Å and visual up to this value. Whenever the identification comes from the Kurucz compilation (1981) or from Kelly, Palumbo (1973), we have added K or KP, respectively.
5. The line shift, observed minus laboratory, in Å.
6. The central line intensity I defined as $I = 100 \times (F(\text{continuum}) - F(\text{line center}))/F(\text{continuum})$.
7. The value of FWHM/observed wavelength, multiplied by 10^4.
8. Remarks : we use the following convention :
   BL : the line is blended with either the preceding or the following one
   RM : a reseau mark affects the line
   (?) : the proposed identification remains doubtful

The identifications were performed on the basis of the multiplet tables of Moore (1968) and of Kelly and Palumbo (1973). The compilation of Kurucz (1981) for the Fe II lines was also used for a number of lines not listed in the previous ones. We finally checked our identifications with the list of Underhill and Adelman (1977) obtained for stars with a similar spectral type and with the list of Altamore *et al.* (1982) derived from the spectrum of KQ Puppis, dominated by Fe II lines.

The precision of the observed line position is limited by the IUE resolution ($\pm$ 0.1 Å and more) and by the difficulty to measure the line center (variable with the type of profile). It is also known that the wavelength calibration of the large aperture experiment can be systematically in error by as much as 45 km/s. Despite that some of the lines display a double structure, it would be noticed that we have reported in tables II and III the position of the whole absorption peak. This topic is treated in the next section. The estimated intensities are uncertain : the usual problem with defining the continuum level in presence of noise is increased by the interorder background level. For these measurements, the local continua were drawn through the highest points in a region of about 200 Å, averaging the noise and neglecting the very noisy overlapping regions.

From the data presented in these tables, we have calculated for all unblended lines of the different ions the following mean quantities :

— Mean heliocentric radial velocities in km/s, measured in SWP and LWR parts of the spectrum.

— Mean FWHM/λ, multiplied by 10^4.

— Edge velocities in km/s measured from the line center for asymmetrical resonance lines,

and we have reported them in table IV, altogether with their standard deviation (σ) and the number of measured lines (n).

The quantities obtained from a small number of lines are evidently less credible.

We can immediately see a systematic shift between the LWR and SWP velocities of about 17 km/s, due to uncertainties in the calibration procedure.

Since we do not detect any interstellar line in the spectra (see next section), it is impossible to recalibrate these velocities and only the relative values are significant. For the same reason, the edge velocities were not taken from the laboratory wavelength but still indicate an expansion of the envelope.

Since the spectra, taken at different epochs, present strong variations, the previous data are only representative of the atmospheric situation in March 1979. When additional lines are observed one year later, essentially excited singly ionized lines, those observed in March 1979 are present in all spectra, thus forming the basic UV spectrum of HD 50138, at a moment of lower excitation. The variations of the mean quantities summarized in table IV, are discussed in the next section for the most important spectral lines.

3. Description of the spectrum.

The ultraviolet spectrum of the Be star HD 50138 presents a great variety of ionization stages, going from neutral N I, O I, Mg I to highly ionized species such as C IV, Si IV. The singly ionized elements dominate the spectrum, mainly Fe II, Ni II and Cr II; Fe III lines, definitely present, are quite rare.

There are only a few emission lines in the UV spectrum of HD 50138 : the Mg II doublet at λ2800 and some Fe II multiplets (62/63, 60, 78) at longer wavelengths. From our data, we can also observe definite, long-term variations, affecting both the absorption and emission features. The absorption lines observed in the spectrum of HD 50138 can roughly be classified into a broad line system and a narrower one, probably originating in different physical regions.

3.1 Broad absorption lines. — Broad and asymmetrical absorption profiles are observed for the resonance lines of C IV and Si IV (N V seems to be absent). Since Si IV and C IV are not expected in spectral types later than B3 and B1, respectively (Marlborough, 1982), the presence of these ions confirms the superionization state in spectral types as late as B8. (Doazan, 1982; Slettebak and Carpenter, 1983). It should be noted that these lines are definitely intense, in spite of the quite low $v \sin i$ (150 km/s) of HD 50138 and do not agree with the correlation proposed by Marlborough (1982) and Slettebak and Carpenter (1983).

The radial velocities of the lines of these ions are affected by a great imprecision since they display a complex profile partially blended with Fe II lines. Nevertheless, the values measured in March 1979, at a period of lower Fe II blending, are the most redshifted among the velocities of the various ions.

Since the profile of Si IV λ1393.8 shows a shortward extension, we attempted to determine the edge velocity from the line center. We derived a value of 580 km/s but the profile seems to be deformed by a Fe II line at λ1392.3 (Kurucz, 1981). This blend is more apparent one year later (see Fig. 1) and the presence of a real blue wing appears to be very spurious. Apparently, the evolution of the Si IV and C IV features with time is essentially due to the intensity variation of the blending Fe II lines. Extreme cases are illustrated in figure 1, where the narrow components are attributed to Fe II lines because they are enhanced at the same moment as are isolated ones (see next section) and are present in only one of the Si IV resonance lines. In our spectra, the usual blending of C IV with Fe III (80) does not occur. No other variation can be detected : among all our spectra, intensities, FWHM remains approximatively the same for both Si IV and C IV.

Other lines, like those belonging to the Fe III (34) or Al III (1) multiplets, show also a broad absorption profile (see Fig. 2) with FWHM intermediate between the previous one and those of the singly ionized elements. The completely different radial velocity of Fe III lines and super-ionized lines, suggests that they are more closely connected with the Fe II lines. Their evolution is illustrated in figure 2.

3.2 THE Mg II RESONANCE DOUBLET. — One of the most striking features in the long wavelength region of the IUE spectrum of HD 50138 is the Mg II resonance doublet, characterized by a P Cygni profile (Fig. 3). Both absorption and emission are well defined and show considerable variations with time. Nevertheless, the emission component is present in all our spectra unlike the Fe II emission which disappears from Nov. 1980. Such line profiles for Mg II are quite uncommon among the Be stars which often show a very sharp absorption on a weak emission, if present at all, as well as for early-type stars (Dachs, 1980; Bruhweiler *et al.*, 1982) as for later type stars (Slettebak and Carpenter, 1983).

The P Cygni profiles of the Mg II doublet observed in HD 50138 resemble those observed in 17 Lep, a binary Be Star (Molaro *et al.*, 1982) or in AB Aur, an Herbig Ae Star (Talavera *et al.*, 1982).

The radial velocities of the absorption lines are similar to those of other singly ionized elements, suggesting a common origin, but no double structure was observed like in other ions.

The narrow blueshifted components seen in the absorption profile are probably due to a blending with Fe II lines, like for Si IV and C IV, masking an eventual double structure.

Our identifications are reported in figure 3. The presence of Mn I λλ2794.8, 2798.3, 2801.1 is also possible.

3.3 SHARP ABSORPTION LINES. — The majority of the spectral features observed in the IUE spectrum of HD 50138 consist of narrow absorption lines of singly ionized elements, mostly those due to Fe II. While these lines are indeed narrower than the previous ones, their FWHM remains quite large (about 100 km/s). Such a large width is not surprising because we suspect that all features of singly ionized elements show a double structure. Among the observations carried out during the period December 1978-March 1979, about 30 % of these narrow lines show a definite doubling, independently of their excitation potential. The two components are of similar intensities and the slight separation (~ 35 km/s), near the resolution limit, cannot easily be detected in all unblended lines. But the greater is the velocity separation between the components (as in the Cr II lines), the more numerous are the lines where such a structure is detected, suggesting it is present for all the singly ionized element features.

In table V, we have reported the velocities of each component, measured from the lines of the LWR part of the spectra obtained in Dec. 1978 and March 1979 and corrected for the earth's motion. If no lines of an ion were present in this spectral range (as Si II, Al II), we used the velocity measured in the SWP spectra corrected for the systematic shift (evaluated from comparison between Fe II lines measured in the two spectra parts and supposing that they do have the same mean velocity). These values are evidently less reliable than those derived from a very few lines (the number of lines is given). A typical value of the standard deviation σ is 7 km/s.

The behavior of some of the Fe II and Cr II lines is illustrated in figure 4 for three epochs (see also Fig. 6). We can see that the separation is greater for the Cr II lines than for the Fe II lines and more important in December 1978 than in March 1979. The relative intensity of the components does not show any significant variation.

The spectrum obtained in February 1979 is unfortunately of lesser quality but shows an intermediate velocity structure between these two epochs.

In the other spectra, obtained at least one year later, no definite evidence of doubling can be seen while a gradual decrease of FWHM is observed. Some values of FWHM/λ($\times 10^4$) are reported in table VI, for a few typical unblended Fe II and Cr II lines measurable at different epochs and indicate a decrease of the width despite some fluctuations.

The variation of the velocity with the ionization potential is shown in figure 7, for three epochs. A net decrease of velocities with an increasing ionization is observed, except for the bluest component measured in the 1978 spectrum. The spectra obtained later (11/80 and 01/82) do not allow to extract conclusive information on this relation.

No similar correlation between the radial velocity and the excitation can be found for the Fe II lines (as illustrated in Fig. 8). Also there is no correlation between the separation of the two components of the profile and the excitation potential.

Because this separation shows variations with the line intensity, we have investigated the velocity difference between the two components against log *gf*. A clear-cut correlation, reported in figure 9a, is observed in December 1978 for the Cr II lines originating from the same excitation level. No such correlation can be derived for the Cr II lines observed in March 1979. As observed in figure 9b the log *gf* dependence is essentially present in the high velocity component, the other one being practically constant.

A variation of the separation due to the superposition of two lines of increasing intensity will affect the two

components equally and cannot explain this result. The same investigation was done for the Fe II lines without any result probably because these lines display a lower velocity separation approaching the resolution limit and are more affected by noise. Principally in the Fe II lines observed in March 1979 where the double structure becomes often spurious, chiefly for the high excitation features. So we preferentially detect a double structure for lines with a low log *gf*, leading to an overestimated measured velocity difference for the Fe II lines.

Because a lot of Fe II lines show asymmetrical profiles extended toward the short wavelengths, we have also investigated the variations of the mean edge velocity with the excitation potential. From the data measured in the images SWP 4557 and LWR 3967 (March 1979), a definite decrease of asymmetry with the increasing excitation potential is observed (Fig. 10). A similar behavior is observed in the spectra taken in Dec. 1978 but it is impossible to compare the values without a precise velocity zero point. It should be noted that, at this epoch, some Cr II lines show an asymmetry in their profiles, not detected later, in March 1979.

But from Feb. 1980, no asymmetry (except sporadic cases) can be observed in the lines of singly ionized elements.

A definite emission is observed for wavelengths greater than λ2700 Å, in the Fe II multiplets 62, 63, 60 and 78. The lines of multiplets 62/63 being close to each other, only a broad emission is seen, while some isolated lines of multiplets 60 and 78, display a highly variable complex structure. The absorption emission profile of one of these lines is illustrated in figure 5 (see also Fig. 6).

In the spectrum taken in Feb. 1980, two new emission features are observed and identified as belonging to Fe II lines. In the subsequent spectra, the emission disappears while the absorption lines of singly ionized elements are progressively enhanced. This intensity increase of weak absorption lines, present from Feb. 1980 to Nov. 1980 is also clearly observed in figures 4 and 5. All these lines belong to singly ionized elements (Fe II, Cr II, Ni II) and a majority of them can be identified as Fe II lines with a low excitation potential near 3 eV. They do not show any significant velocity shift in comparison with the « permanent » features.

In January 1982, these lines are no longer detected : the observed features are those of March 1979.

Finally, observations of the lines due to the singly ionized elements may be divided into broad classes of similar properties (in spite of some fluctuations), which correspond to the different periods of observations.

a) period from Dec. 1978 to March 1979
- — double structure in absorption lines, progressively vanishing with time (large FWHM)
- — net asymmetry of low excitation lines
- — variable Fe II emission

b) period from Feb. 1980 to Nov. 1980
- — absence of a double structure for the absorption lines
- — no asymmetry
- — progressive enhancement of weak lines
- — disappearance of Fe II emission (still present in Feb. 1980)

c) period of Jan. 1982
- — no double structure of absorption lines (low FWHM)
- — no asymmetry
- — no Fe II emission
- — disappearance of the weak lines.

3.4 THE INTERSTELLAR LINES. — We have not been able to detect any interstellar feature in our data. Furthermore no systematic difference between the FWHM or the radial velocities of the 0.00 eV absorption lines and the excited ones can be found, at any epoch of observation.

The double structure reported for the singly ionized elements cannot be attributed to the presence of an interstellar component because it also appears in lines originating from excited levels. So, we conclude that either the interstellar lines are weak, or their radial velocity is close to that of the circumstellar absorption lines. We have also tried to detect the strongest CO lines, perhaps associated with the presence of Si II (2) as suggested by Tarafdar (1983) but the blending with Fe II lines does not permit to test this.

In any case, the interstellar extinction toward HD 50138 is small, as reported by Houziaux and Andrillat (1976), from the weakness of the λ2200 Å feature observed with TD1. The IUE low dispersion spectra lead to the same conclusion.

4. Discussion.

4.1 EVIDENCE FOR AN OUTBURST IN 1978-1979. — One of the most striking characteristics of the ultraviolet spectrum of HD 50138 is the presence, during the December 1978-March 1979 period of a double structure in the lines of singly ionized elements.

Satellites were also reported for Hγ by Merrill (1952) and Doazan (1965) with a velocity of about 100 km/s. But their behavior was completely different : they are only present during a few days and alternatively on the red and violet sides of the lines. Molaro *et al.* (1982) have reported a similar observation in the spectrum of the Be star 17 Lep : in the visible the components are only present during outburst while in the ultraviolet they seem to be a permanent feature. Having no simultaneous observations of HD 50138 in the two spectral ranges, it is impossible to find any relation between the Balmer satellites and the metallic ones. Nevertheless, the Balmer lines are probably formed in deeper regions where violent acceleration and deceleration can occur (Doazan, 1965).

In spite of the absence of a precise wavelength calibration, the low outflow velocity component remains nearly constant in all our spectra for a given ion, suggesting that the intermittent component is the most displaced one.

These observations may be explained by assuming that the wind consists of two coexisting components having different velocities. One of them is always present and observed at nearly the same velocity at every epoch whereas the other one is the consequence of an outburst that occurred in December 1978 (or before).

The persistence during at least three months of this double structure in the line profiles is incompatible with an interpretation of their formation in two distinct expanding rings (i.e. regions of greater density).

From December 1978 to March 1979 the velocity separation between the two components shows a net decrease, suggesting that the latest expelled component of the wing is progressively decelerated. An outward deceleration was already suggested by Doazan (1965) from visual observations.

As seen in figure 9, the outflow velocity of the singly ionized elements decreases with the decreasing ionization potential. The velocities of neutral and twice ionized elements (Mg I, N I, Fe III) are in agreement with this tendency. So, the envelope is stratified with an outward decreasing ionization and consequently an outward decreasing FWHM (see Table IV) indicating a decrease of the velocity turbulence and/or a decrease of the rotation velocity of the envelope. The correlation between the edge velocity and the ionization potential (Table IV) seems also in agreement with this interpretation : the deepest lines (Si II) show the more extended violet wings and in December 1978, more lines (as Cr II) display a violet asymmetry indicating higher outflow velocities. On the contrary, no stratification with the excitation potential can be detected, as illustrated in figure 8, probably due to a weak temperature variation in the region where the Fe II lines are formed.

If the characteristics of the low velocity component of the wind seem unchanged at every epoch, strong variations affect the high velocity one. In December 1978 it fails to show any definite ionization stratification while 3 months later it does as in the low velocity component (Fig. 7).

Also in December 1978, the high velocity component of the Cr II lines displays a log *gf* dependence, in agreement with a decelerated wind in which the strongest lines are formed further away from the stellar core. This correlation, absent in the low velocity feature, disappears in the spectra taken in March 1979. So, the evolution between Dec. 1978 and March 1979 of the envelope surrounding HD 50138 is essentially due to the newly outburst part of the wind which progressively dissipates in the old one, getting similar physical properties.

According to this model, we do expect in Dec. 1978 a lower emission in the high velocity part of the wind formed nearest the star (Viotti and Koubsky, 1982), than in the low velocity one, whereas, in March 1979, the emission must have approximatively the same intensity for both components. This is in good agreement with the P Cygni profiles observed in Dec. 1978 where the violet emission was absorbed by the high velocity absorption feature and with the broad emission line, probably due to both parts of the wind, observed in March 1979.

As previously noticed the emission features are only present in the long wavelength range, probably because of the gradual decrease of continuum with increasing wavelength : some lines (as Fe II 2) with the same upper level and similar log *gf* as Fe II 60 or 78 are only observed in absorption.

The spectra obtained during 1980 also show an interesting evolution : the progressive enhancement of weak lines of singly ionized elements. At this epoch, only one component of the wind is still present and shows the characteristics of the low velocity one that was observed more than one year before.

Because the central intensity of some of the new lines becomes as large as the other neighbouring lines, this evolution is due to an increase of the excitation rather than to an increase of the continuum.

Unfortunately, the lack of observations during more than one year does not allow us to know whether this excitation is a consequence of the outburst or not.

4.2 A FLUORESCENCE MECHANISM FOR Mg II. — Some lines are affected by a different behavior : it is the case of C IV and Si IV which probably originate from a completely different region. On the contrary the Fe III absorption lines have properties more common with those of singly ionized element lines in spite of the fact that they seem to be formed in a deeper region.

The Mg II emission line profiles, unusual in Be stars, seem also uncorrelated with the Fe II emission. Bruhweiler *et al.* (1982), have shown that, in some Be stars, the emission in the Mg II h and k lines contains a definite contribution caused by a fluorescence mechanism driven by Lyβ. In the case of HD 50138, the profile will be composed of a broad emission plus an asymmetrical absorption line whose blue wing (if present) may absorb the blue part of the emission. With the rapid conversion of Lyβ in Hα plus photons in the $2\,^2S - 1\,^2S$ continuum (Osterbrock, 1974), the presence of a Bowen mechanism implies that the Mg II emission arises in the same physical region as the hydrogen recombination spectrum. So we might expect comparable widths. The mean halfwidth of Hβ and Hγ emission components is about 4.7 Å (Houziaux, 1960 and Doazan, 1965). If we suppose that the Mg II λ2803.3 emission is centered on the stellar wavelength, the corresponding halfwidth is found to be 5.1 Å (in LWR 3967), nearly the same as the previous value.

Another proof which supports the fluorescence mechanism is the presence of O I λ8446 in emission, as suggested by Bruhweiler *et al.* (1982). Nevertheless, the presence of O I λ1302 in absorption and the observed profiles of Mg II (3) show that a more complete and quantitative approach is necessary in order to determine the relative importance of radiative recombination and fluorescence mechanism for both O I and Mg II.

5. Conclusions.

The absorption features observed in the ultraviolet spectrum of HD 50138 can be classified into at least two line systems, which probably originate in different regions : a broad line system due to the high ionization lines (Si IV, C IV) and a narrower one which essentially consists of lines belonging to singly ionized elements.

The lines of these elements seem to show that the envelope surrounding HD 50138 is decelerated with an outward decreasing ionization. They also suffer long-term variations, which are characterized by a double absorption line profile structure in 1978-79 and an enhancement of weak

absorption lines in 1980 which vanishes later. We interpreted these observations with a two component stellar wind, one component of which outburst in Dec. 1978.

We have also suggested that a fluorescence mechanism may contribute to the formation of the emission in the Mg II doublet.

An accurate list of line identifications in the UV spectrum of HD 50138 has been provided as a reference table for future investigations.

Acknowledgements.

I wish to thank Prof. L. Houziaux for suggesting and supervising this work, Dr. J. Surdej for a careful reading of the manuscript and Dr. R. Viotti, the referee, for many helpful comments.

We are also grateful to the Centre de Données Stellaires (CDS) at Strasbourg for a complete bibliography on HD 50138.

References

ALLEN, D. A. : 1973, *Monthly Notices Roy. Astron. Soc.* **161,** 145.
ALTAMORE, A., GIANGRANDE, A., VIOTTI, R., 1982, *Astron. Astrophys. Suppl. Ser.* **49,** 511.
ANDRILLAT, Y., HOUZIAUX, L. : 1972, *Astrophys. Space Sci.* **18,** 324.
BRUHWEILER, F. C., MORGAN, T. H., VAN DER HUCHT, K. A. : 1982, *Astrophys. J.* **262,** 675.
DACHS, J. : 1980, 2d Eur. IUE Conf., ESA-SP157, 139.
DOAZAN, V. : 1965, *Ann. Astrophys.* **28,** 1.
DOAZAN, V., 1982, in *B stars with and without emission lines* (NASA, SP456, Washington), p. 377.
HOUZIAUX, L. : 1960, *J. Observateurs* **43,** 217.
HOUZIAUX, L., ANDRILLAT, Y. : 1976, *IAU Symp.* **70,** 87.
KELLY, R. L., PALUMBO, L. J. : 1973, *Atomic and ionic emission lines below 2000* Å (NRL, Washington).
KUAN, P., KUHI, L. V. : 1975, *Astrophys. J.* **199,** 148.
KURUCZ, R. L. : 1981, *SAO Special Report* No. 390.
MARLBOROUGH, J. M. : 1982, *IAU Symp.* **98,** 361.
MERRILL, P. : 1931, *Astrophys. J.* **73,** 348.
MERRILL, P. : 1952, *Astrophys. J.* **116,** 501.
MOLARO, P., SELVELLI, P. L., STALIO, R. : 1982, *IAU Symp.* **98,** 437.
MOORE, C. E. : 1968, *NBS Circ.* No. 488.
OSTERBROCK, D. E. : 1974, *Astrophysics of gaseous nebulae* (San Francisco, Freeman).
SITKO, M. L., SAVAGE, B. D., MEADE, M. R. : 1981, *Astrophys. J.* **246,** 161.
SLETTEBAK, A., CARPENTER, K. G. : 1983, *Astrophys. J. Suppl. Ser.* **53,** 869.
SWINGS, P., STRUVE, O. : 1940, *Publ. Astron. Soc. Pacific* **52,** 294.
TALAVERA, A., CATALA, C., CRIVELLARI, L., CZARNY, J., FELENBOK, P., PRADERIE, F. : 1982, 3d Eur. IUE Conf. ESA-SP176, 99.
TARAFDAR, S. P. : 1983, *Monthly Notices Roy. Astron. Soc.* **204,** 1081.
UNDERHILL, A. B., ADELMAN, S. J. : 1977, *Astrophys. J. Suppl.* **34,** 309.
VIOTTI, R., KOUBSKY, P. : 1976, *IAU Symp.* **70,** 99.
VIOTTI, R., GIANGRANDE, A., ALTAMORE, A., CASSATELLA, A., FRIEDJUNG, M., MURATORIO, G., RICCIARDI, O. : 1980, 2d Eur. IUE Conf., ESA-SP157, 39.

1985A&AS...60..373H

TABLE I. — *High resolution IUE observations of HD 50138.*

Image	Camera	Date	exposure (s)	aperture	illustration
3225	LWR	78/12/21	4500	S	
3227	LWR	78/12/21	2100	S	(1)
3662	SWP	78/12/21	4800	S	(1)
3795	LWR	79/02/18	1800	S	(2)
3967	LWR	79/03/09	980	L	(3)
4295	SWP	79/02/18	1800	S	
4557	SWP	79/03/09	1800	L	(3)
6967	LWR	80/02/22	900	L	(4)
7889	SWP	80/02/07	6000	S	
8007	SWP	80/02/22	2700	L	(4)
9358	LWR	80/11/21	900	L	(7)
9806	SWP	80/08/16	6000	S	
10450	SWP	80/10/22	6000	S	(6)
10649	SWP	80/11/21	2400	L	(7)
12310	LWR	82/01/09	900	L	
12322	LWR	82/01/11	1320	L	(8)
15993	SWP	82/01/09	2400	L	
16017	SWP	82/01/11	2400	L	

TABLE V. — *Velocity structure of the absorption lines*

	21 DEC 78				09 MAR 79			
	V1	V2	ΔV	n	V1	V2	ΔV	n
AlII	11	66	55	2	38	72	34	3
CrII	-23	43	66	18	26	68	42	19
MnII	-11	36	47	2	19	56	37	1
MgII		24		2		46		2
NiII	-21	28	49	8	21	49	28	6
FeII	-19	30	49	36	17	49	32	31
SiII	-25	28	52	2	3	43	40	2

TABLE IV. — *Mean quantities for unblended lines.*

Ion	V_{SWP}	σ	n	V_{LWR}	σ	n	FWHM/λ	σ	n	V_{edge}	σ	n
NI	20	14	3				2.9		2			
MgI				48		1	1.8		1			
AlII	41	5	4				3.4		2			
CrII				48	13	28	3.0	1.0	22			
MnII				52	6	3						
MgII				46	6	4	6.3 *	1	2	-217 *		2
NiII	13	16	18	31	13	18	3.9	0.8	30	-107	9	4
FeII LE	10	12	55	27	12	50	3.8	0.7	56	-142	15	17
FeII	11	15	111	27	13	134	3.5	0.7	121			
SiII	11	15	6				4.1	1.4	3	-185		2
FeIII	4	13	3				6.3		2			
SiIV	50		2				14.0 *		2	-580 *		1
CIV	75		1				12.0 *		1			

* very uncertain because of a possible blending with FeII lines - see text.

TABLE VI. — *Long term variation of FWHM/λ ($\bar{\sigma} \sim 0.5$).*

	DEC 78	FEB 79	MAR 79	FEB 80	NOV 80	JAN 82
FeII LE	4.3	3.5	3.7	2.9	2.2	2.4
FeII HE	3.5	2.7	2.7	2.4	2.2	2.0
CrII	3.7	2.5	2.7	2.3	2.2	1.7

TABLE II. — *Absorption lines in SWP 4557.*

OBS.WL	LAB.WL	ION	MULT	SHIFT	INT	FWHM	REMARKS
1253.8	53.47	NI II	KP		100	7.2	
	53.79	S II	1				
1256.7	56.43	FE II	K	0.27	63	4.8	(?)
1259.6	59.53	S II	1		100		BL
	59.64	FE II	K				BL
1260.7	60.42	SI II	4		100		BL
	60.54	FE II	9				BL
1264.9	64.74	SI II	4		100	12.8	
	65.02	SI II	4				
1266.8	66.69	FE II	9	0.11	95	3.2	
1267.6	67.44	FE II	9	0.16	100	2.8	
1269.3	69.04	FE II	K		48	4.0	
	69.35	FE II	K				
1272.1	72.00	FE II	9	0.10	97		BL
1272.8	72.64	FE II	9	0.16	97		BL
1275.2	75.15	FE II	9	0.05	95	2.8	
1275.9	75.80	FE II	9	0.10	94	3.1	
1277.7	77.25	C I	7		97	5.4	
	77.28	C I	7				
	77.51	C I	7				
	77.55	C I	7				
	77.67	FE II	9				
	77.72	C I	7				
1279.2	79.10	FE II	K	0.10	35	2.4	
1279.5					46	2.3	
1280.7	80.33	C I	5		48	5.4	BM.(?)
	80.59	C I	5				
	80.85	C I	5				
1286.5	86.38	TI III	2	0.12	30	3.8	
1290.3	90.21	FE II	88	0.09	56	3.1	(?)
1291.8	91.59	FE II	87		55	2.3	
	91.64	TI III	2				
1293.3	93.26	TI III	2	0.04			
1294.9	94.54	SI III	4		67		
	94.67	TI III	2				
	94.67	TI III	1				
	94.91	FE II	87				
1296.2	95.88	TI III	1		53		
	96.08	FE II	86				
1299.2	98.67	TI III	1		67	11.5	
	98.89	SI III	4				
	98.95	TI III	1				
	98.96	SI III	4				
1301.4	01.15	SI III	4	0.25	45		BL
1302.3	02.17	O I	2	0.13	100	7.7	BL
1304.7	03.32	SI III	4	0.48	94	9.9	
	04.47	P II	2				
	04.68	P II	2				
	04.86	O I	2				
1305.8	05.48	P II	2	0.32	81		BL
1306.2	06.03	O I	2	0.17	100		BL
1309.3	08.87	NI II	10		100	5.4	
	09.28	SI II	3				
1311.0	10.57	N I	13		64	4.6	
	10.70	P II	2				
	10.97	N I	13				
	11.06	FE II	K				
1316.6	16.49	FE II	K	0.11	44	3.1	BL
1317.3	17.22	NI II	10	0.08	94	3.8	BL
1324.0	23.86	C II	11		48	12.3	
	23.91	C II	11				
	23.96	C II	11				
1326.8	26.57	N I	11	0.23	28	2.2	
1328.1	27.92	N I	11		26		
	27.93	N I	11				
1329.3	29.09	C I	4		46	4.4	BL
	29.10	C I	4				BL
	29.12	C I	4				BL
1329.8	29.58	C I	4		33	3.0	BL
	29.60	C I	4				BL
1334.5	34.53	C II	1		100		BL
	34.87	P III	1				BL.(?)
1335.7	35.66	C II	1		100		BL.BM
	35.71	C II	1				BL
1348.8	48.54	SI II	7	0.26	35	3.0	
1350.5	50.06	SI II	7		32	11.1	
	50.52	SI II	7				
	50.66	SI II	7				
1353.0	52.64	SI II	7		51	3.7	
	53.02	FE II	K				
1353.9	53.72	SI II	7	0.18	32		
1359.1	58.99	NI II	15	0.11			
1362.8	62.77	FE II	182	0.03	51		
1363.7	63.62	FE II	K	0.08	52		
1364.8	64.57	FE II	103	0.23	58	4.4	
1368.4	68.09	FE II	KP		42	8.1	BM
	68.26	FE II	K				
1370.2	70.14	NI II	6	0.06	87	4.4	
1371.3	71.02	FE II	KP	0.28	44	3.0	
1372.5	72.29	FE II	K	0.21			
1374.3	74.08	NI II	9	0.22			
1375.4	75.17	FE II	KP	0.23			
1377.1	76.67	FE II	KP		45	5.2	
	77.01	NI II	KP				
1378.3	78.28	FE II	K		36	5.7	
	78.35	FE II	K				
1379.8	79.47	FE II	KP		61	5.0	FE II BL
	79.67	AL III	KP				
1381.5	81.25	FE II	152		58	5.7	
	81.29	NI II	8				
1383.7	83.58	FE II	KP	0.12	38	2.1	
1387.4	87.22	FE II	KP	0.28			
1392.3	92.15	FE II	K	0.15	39		BL
1394.0	93.76	SI IV	1	0.24	87	14.3	BL FE II
1397.8	97.57	FE II	350	0.23	20	3.6	
1398.8	98.63	FE II	K	0.17	26		
1399.2	99.03	NI II	8		51	2.7	
	99.06	FE II	K				
1403.2	02.77	SI IV	1	0.43	69	13.6	BL
1404.2	04.12	FE II	K	0.08	40		BL
1405.8	05.60	FE II	KP		56	6.4	
	05.80	FE II	KP				
1408.7	08.48	FE II	KP	0.22	50	3.6	
1409.4	09.07	SI II	13.02		39	2.9	
	09.31	FE II	K				
1410.3	09.90	SI II	13.02		33		
	10.22	SI II	13.02				
1411.2	11.07	NI II	KP	0.13	46	2.9	
1412.2	11.93	N I	10		59	2.9	
	11.94	N I	10				
	11.95	N I	10				
1413.0	12.83	FE II	47		72	3.6	
	12.87	NI II	KP				
1419.1	18.85	FE II	KP	0.25	44	3.6	
1421.1	20.91	FE II	KP	0.19	45		(?)
1422.8	22.53	FE II	K	0.27	46	2.1	
1424.3	24.05	FE II	47	0.25	41		BL
1424.9	24.72	FE II	47	0.18	62		BL
1435.1	34.67	FE II	K		68	6.9	
	34.99	FE II	KP				
1439.7	39.43	FE II	KP	0.27	40	2.8	
1442.9	42.75	FE II	KP	0.15	41	4.1	FE II BL
1448.7	48.35	FE II	K		42	4.8	
	48.39	FE II	KP				
1455.0	54.96	NI II	7	0.04	67	3.4	
1459.5	59.31	FE II	193	0.19			
1465.1	65.04	FE II	193	0.06	43	4.8	FE II BL
1467.6	67.27	NI II	KP		64		BL
	67.69	NI II	KP				BL
1468.1	67.85	NI II	6	0.25	64		BL
1473.9	73.63	FE II	193	0.07	56		
1483.7	83.55	FE II	K		42	5.5	
	83.64	FE II	K				
1485.7	85.19	NI II	KP		48	6.7	
	85.30	NI II	KP				
1492.8	92.63	N I	4		97	4.0	
	92.82	N I	4				
1494.9	94.68	N I	4		97	3.3	
	94.77	FE II	K				
1500.7	00.44	NI II	7	0.26	64	2.7	
1502.5	02.16	NI II	KP	0.35	50	2.7	
1516.0	15.79	NI II	KP		50		BL
	15.83	NI II	KP				BL
1516.3	16.05	NI II	KP		34		BL
	16.22	NI II	KP				BL
1526.8	26.72	SI II	2	0.08	100		
1533.5	33.44	SI II	2	0.06	96	7.3	
1536.9	36.72	NI II	KP		54		
	36.75	NI II	KP				
	36.76	NI II	KP				
1548.7	48.19	C IV	1	0.51	73	12.0	
1551.3	50.77	C IV	1	0.53	76	14.0	BL FE II
1559.0	58.54	FE II	46		94	7.7	
	58.71	FE II	46				
	59.11	FE II	45				
1561.2	60.31	C I	3		54	13.5	
	60.70	C I	3				
	61.29	C I	3				
	61.40	C I	3				
1563.9	63.79	FE II	45	0.11	93	4.5	
1565.6	65.36	FE II	46	0.24	52	4.5	
1567.0	66.83	FE II	44	0.17	94	3.9	
1568.2	68.03	FE II	45	0.17	69	3.9	
1569.8	69.67	FE II	44	0.13	94		BL
1570.4	70.25	FE II	45	0.15	94		BL
1571.4	71.01	FE II	K		32	3.9	
	71.06	FE II	K				
1574.0	73.83	FE II	45	0.17	89	3.9	
1575.1	74.78	FE II	44		92	6.5	
	74.93	FE II	45				
1577.3	77.16	FE II	45	0.14	86	3.8	
1580.7	80.63	FE II	44	0.07	89	3.8	BM
1585.2	84.95	FE II	44	0.25	88	4.4	
1588.5	88.29	FE II	44	0.21	88	3.1	
1602.9	02.52	FE II	K	0.38	53	7.5	(?)
1605.5	05.32	FE II	KP	0.18	56		BL
1606.1	05.91	NI II	KP	0.19	55		BL
1608.6	08.45	FE II	8	0.15	94	4.4	
1611.2	10.93	FE II	43	0.27	84	5.6	BM
1612.9	12.81	FE II	43	0.09	98	6.3	FE II BL
1618.6	18.46	FE II	8	0.14	95	3.8	
1621.8	21.68	FE II	8	0.12	94	5.0	FE II BL
1623.2	23.10	FE II	43	0.10	81	3.1	
1625.8	25.52	FE II	43		95	6.3	BM
	25.92	FE II	8				
1629.3	29.15	FE II	8	0.15	94	4.2	

TABLE II *(continued)*.

OBS.WL	LAB.WL	ION	MULT	SHIFT	INT	FWHM	REMARKS
1631.3	31.12	FE II	8	0.18	81	3.6	
1632.8	32.67	FE II	43	0.13	88	3.6	
1634.3	33.91	FE II	43		61	5.5	
	34.35	FE II	8				
1635.5	35.39	FE II	68	0.11	86	4.2	
1637.6	37.40	FE II	42	0.20	92	3.6	
1639.6	39.40	FE II	8	0.20	81		BL
1640.3	40.17	FE II	43	0.13	89		BL
1641.9	41.76	FE II	68	0.14	77	3.0	
1643.8	43.59	FE II	42	0.21	97	3.6	
1646.3	46.19	FE II	68	0.11	75		
1647.4	47.16	FE II	68	0.24	75	3.0	
1649.6	49.44	FE II	42		89	4.2	
	49.58	FE II	68				
1650.9	50.71	FE II	68	0.19	77	3.6	
1654.6	54.10	FE II	68		78	4.8	RM
	54.48	FE II	42				
1657.3	57.05	FE II	42	0.25	67		
1658.9	58.76	FE II	41	0.12	83		BL
1659.7	59.49	FE II	40	0.21	92		BL
1661.6	61.35	FE II	41	0.25	44	3.0	
1663.4	63.23	FE II	40	0.17	78	3.6	
1666.2	67.91	FE II	K	0.29	30	2.4	
1670.8	70.75	FE II	40		100	11.5	
	70.81	AL II	2				
1673.5	73.47	FE II	102	0.03	93		BL
1674.7	74.26	FE II	41		85		BL
	74.72	FE II	40				BL
1677.1	76.87	FE II	41	0.23	58	3.6	
1678.1	77.85	FE II	KP	0.25	35		
1679.5	79.39	FE II	102	0.11	73	3.6	
1681.3	81.12	FE II	KP	0.18	66	4.2	
1686.1	85.95	FE II	41	0.15	81		BL
1686.6	86.46	FE II	40	0.14	84		BL
1688.6	68.28	FE II	102		55	4.2	
	88.40	FE II	41				
1690.0	89.82	FE II	85	0.18	43	1.8	
1691.1	90.78	FE II	85	0.32	53		BL
1691.5	91.27	FE II	41	0.23	79		BL
1692.8	92.49	FE II	38		54	2.4	
	92.52	FE II	K				
1694.2	93.96	FE II	41	0.24	58		
1697.0	96.80	FE II	38	0.20	81	4.2	
1698.5	98.19	FE II	40		35	4.8	
	98.43	FE II	K				
1699.5	99.20	FE II	85	0.30	35		
1702.2	01.95	FE II	85		95	4.2	RM
	02.04	FE II	38				
1703.5	03.41	NI II	5	0.09	42		
1704.9	04.65	FE II	39	0.25	42	4.7	
1706.4	06.18	FE II	38	0.22	51	4.7	
1707.8	07.41	FE II	64	0.39	43		
1708.8	08.63	FE II	38		87	2.9	
	08.66	FE II	85				
1709.8	09.66	FE II	64	0.12	85	3.5	
1712.0	11.66	FE II	KP	0.34	40	2.9	
1713.2	13.00	FE II	38	0.20	96	4.7	
1716.8	16.57	FE II	39	0.23	55	3.5	
1718.3	18.12	FE II	38	0.18	49		
1720.8	20.62	FE II	38	0.18	85		
1722.7	22.43	FE II	KP	0.37	40		
1725.1	24.85	FE II	39		82	4.7	
	24.97	FE II	37				
1726.6	26.39	FE II	38	0.21	85	3.4	
1731.2	31.04	FE II	110	0.16	33	3.4	
1735.2	34.90	NI II	KP		42	2.9	RM
	35.14	NI II	KP				
1741.8	41.56	NI II	5	0.24	75	3.4	
1742.9	42.72	N I	9		45	2.9	
	42.73	N I	9				
1745.5	45.25	N I	9		30	2.9	
	45.26	N I	9				
1746.9	46.82	FE II	101	0.08	70	4.0	
1748.4	48.30	NI II	5	0.10	66	3.4	
1752.1	51.92	NI II	4	0.18	65	2.9	
1755.0	54.81	NI II	4	0.19	42	2.9	
1758.6	58.31	FE II	K	0.29			
1761.5	61.38	FE II	101	0.12	71		
1764.3	63.91	AL II	5		46	4.7	
	63.95	AL II	5				
1766.2	65.82	AL II	5	0.38	37	3.1	
1768.2	67.73	AL II	5	0.47	33		
1772.7	72.52	FE II	99	0.18	69	4.0	
1774.2	73.96	NI II	3	0.24	33		
1781.6	81.34	FE II	KP				
	81.53	FE II	KP				
1785.3	85.26	FE II	191	0.04	59	3.3	
1786.8	86.74	FE II	191	0.06	57	2.8	
1788.3	88.00	FE II	191		55	6.1	
	88.50	NI II	5				
1793.5	93.37	FE II	99	0.13	57	3.9	
1798.4	98.16	FE II	142	0.24	35	3.9	
1804.8	04.48	NI II	2	0.32	43	3.9	
1808.3	08.01	SI II	1	0.29	82	3.9	
1809.6	09.32	FE II	142	0.28	29		
1817.1	16.94	SI II	1	0.16	78		BL
1817.8	17.42	SI II	1				BL.RM
1818.8	18.51	FE II	66	0.29	39	4.4	
1822.4	22.15	FE II	66	0.25	27	2.2	
1824.2	23.89	FE II	KP	0.31	22		
1827.1	26.99	FE II	65	0.11	20		
1828.2	27.74	FE II	66	0.46	22		
1836.0	35.87	FE II	98	0.13	47	5.9	BL?
1842.1	41.70	FE II	65	0.40	38		FE II BL
1846.9	46.58	FE II	96	0.32	38	3.8	
1848.9	48.77	FE II	141	0.13	28		
1858.4	58.03	AL II	4	0.37	33	3.8	
1860.1	59.74	FE II	65		62	5.4	
	60.04	FE II	97				
1863.0	62.30	AL II	4		71	10.3	
	62.79	AL III	1				
1864.9	64.74	FE II	126	0.16	58	2.7	
1877.0	76.83	FE II	97	0.17	66		BL
1877.7	77.46	FE II	125	0.24	70		BL
1888.8	88.73	FE II	125	0.07	55	3.2	
1895.7	95.46	FE III	34	0.24	71	6.3	BL FE II 124
1899.2	98.87	FE III	KP	0.33	21		
1910.8	10.67	FE II	124	0.13	19		
1914.2	14.06	FE III	34	0.17	65	6.3	
1926.4	26.30	FE III	34	0.10	73	6.3	
1937.1	36.80	FE II	96	0.30	23		

TABLE III. — *Absorption lines in LWR 3967.*

OBS.WL	LAB.WL	ION	MULT	SHIFT	INT	FWHM	REMARKS
2011.2	10.69	FE II	122	0.51	68	3.0	
2025.9	25.58	CR II	2		100	5.0	
	25.82	MG I	2				
2032.8	32.41	FE II	94	0.39	54		
2040.9	40.69	FE II	93	0.21	64	4.0	
2044.3	43.78	FE II	K	0.52	45	4.5	
2051.4	51.03	FE II	93	0.37			
2055.9	55.59	CR II	1	0.31	100		RM
2062.2	61.54	CR II	1	0.66	100	6.0	BL FE II K
2064.0	63.67	FE II	92	0.33	65	2.5	
2066.1	65.46	FE II	109		81	3.0	
	66.01	CR II	1				
2068.6	67.92	FE II	137		62	5.0	
	68.02	FE II	K				
2079.3	78.76	NI II	16	0.54	65	4.4	
2081.1	80.84	NI II	16	0.26	67	2.4	
2087.9	87.53	FE II	108	0.37	66	3.2	
2097.8	97.41	FE II	K		48	5.4	
	97.51	FE II	80				
2136.7	36.52	FE II	249	0.18			
2162.1	61.16	FE II	370		55	8.1	
	61.31	FE II	370				
	61.31	FE II	227				
	62.02	FE II	90				
2165.9	65.55	NI II	13	0.35	100	4.8	
2169.4	69.10	NI II	13	0.30	100	4.3	
2175.3	74.70	NI II	14		83	6.2	RM
	75.16	NI II	13				
2177.6	77.20	NI II	KP	0.40	73	3.3	
2179.7	79.46	NI II	12	0.24	50	5.2	
2184.9	84.61	NI II	13	0.29	88	5.2	
2201.8	01.41	NI II	13	0.39	78	4.8	
2207.0	06.71	NI II	13	0.29	81	4.8	RM
2210.8	10.38	NI II	13	0.42	75	3.8	
2216.8	16.48	NI II	12	0.32	92	5.0	
2220.8	20.39	FE II	118	0.41	75	5.0	BL
2221.4	21.16	FE II	168	0.24	63		BL
2223.3	22.95	NI II	12	0.35	90	5.5	RM
2225.2	24.88	NI II	12	0.32	89	4.5	
2226.8	26.34	NI II	12	0.46	89	4.0	
2234.3	33.92	FE II	118	0.38	68	3.1	
2245.7	45.51	FE II	365	0.19	51	2.2	
2247.8	47.69	FE II	365	0.11	63		
2249.6	49.06	FE II	365		76	4.4	
	49.18	FE II	365				
	49.18	FE II	5				
2253.9	53.86	NI II	12	0.04			
2256.2	55.69	FE II	365	0.51			
2260.3	60.08	FE II	4		88		
	60.23	FE II	5				
2264.9	64.46	NI II	12	0.44	84	4.0	
2266.5	65.99	FE II	5	0.51	46		
2268.1	67.58	FE II	4	0.52	64	4.4	
2270.6	70.21	NI II	12	0.39	82	4.0	
2284.2	83.99	FE II	132		52	6.7	
	84.22	FE II	105				
2286.4	86.39	FE II	396	0.31	45		BL
2287.6	87.08	NI II	22	0.52	73		BL
2292.2	91.85	FE II	156	0.35	45		
2294.2	93.77	FE II	184	0.43	42	2.6	
2297.5	97.14	NI II	11				
	97.49	NI II	11				
	98.27	NI II	11				
2303.2	02.98	NI II	11	0.32	93	4.3	
2313.3	12.91	NI II	58	0.39	66	4.8	
2316.4	16.03	NI II	11	0.37	88	4.8	
2327.7	27.39	FE II	3	0.31	84	4.3	
2331.7	31.31	FE II	35	0.39	79		BL
2333.2	32.80	FE II	3	0.20	87		BL
2335.2	34.59	NI II	20	0.61	63	3.0	
2338.2	38.00	FE II	3	0.20	82	4.3	
2339.9	39.41	FE II	105	0.49	26	3.4	
2341.6	40.95	FE II	166	0.65	44	3.8	(?)
2344.2	43.49	FE II	3		100	7.7	
	43.96	FE II	35				
	44.65	FE II	3				
2345.8	45.44	NI II	11	0.36	85	3.8	
2348.6	48.12	FE II	36		89	4.7	
	48.30	FE II	3				
2351.5	51.20	FE II	165	0.30	63	3.0	
2355.1	54.88	FE II	35		68	6.4	
	55.22	FE II	165				
2359.5	59.11	FE II	3		85		BL
	59.11	FE II	165				BL
	59.59	FE II	165				BL
2360.5	60.00	FE II	35		80		BL
	60.29	FE II	36				BL
2362.4	62.02	FE II	35	0.38	71	4.3	
2365.2	64.82	FE II	3		88	6.4	
	65.05	FE II	K				
2369.0	68.59	FE II	36	0.41	82	4.3	RM
2370.9	70.49	FE II	35	0.41	81	3.4	
2374.2	73.73	FE II	2	0.47	94	3.8	
2375.6	75.19	FE II	36		80		
	75.43	NI II	21				
2379.5	79.27	FE II	36	0.23	76	6.4	FE II BL
2381.2	80.76	FE II	3	0.44	82		BL
2382.4	82.03	FE II	2	0.37	97		BL+FE II 35
2383.6	83.06	FE II	2		74		BL
	83.24	FE II	36				BL
2384.8	84.39	FE II	36		77		
	84.99	FE II	35				
2388.9	88.63	FE II	2		85	6.4	RM
	88.99	FE II	K				
2391.9	91.48	FE II	35	0.42	65	3.8	
2395.5	95.42	FE II	2		100	8.5	
	95.63	FE II	2				
2399.6	99.24	FE II	2		92	5.1	BL
	99.24	FE II	36				BL
2400.7	00.27	FE II	181		71		BL
	00.34	FE II	244				BL
2402.8	02.60	FE II	36	0.20	69	5.5	FE II BL
2405.0	04.43	FE II	2		87	6.0	
	04.88	FE II	2				
2407.2	06.66	FE II	2	0.54	83	4.7	
2410.9	10.52	FE II	2	0.38	90		BL
2411.6	11.06	FE II	2	0.54	83		BL
2413.7	13.31	FE II	2	0.39	83	5.1	
2416.6	16.13	NI II	20	0.47	72		
2418.3	17.86	FE II	244	0.44	71	3.4	
2424.7	24.14	FE II	180		68		
	24.58	FE II	180				
2428.8	28.37	FE II	300		76		BL
	28.79	FE II	301				BL
2430.4	30.07	FE II	180		72		BL
	30.18	FE II	301				BL
2432.9	32.26	FE II	180		73	5.3	
	32.70	FE II	321				
	32.87	FE II	321				
2435.2	34.73	FE II	321				RM
	34.94	FE II	180				
2437.8	37.63	FE II	375	0.19	45		BL
2438.4	38.01	FE II	K		52		BL
	38.05	FE II	K				BL
2439.7	39.30	FE II	209	0.40	82	3.7	
2440.9	40.42	FE II	300	0.48	53	2.4	
2444.9	44.52	FE II	148	0.38	80	3.7	
2446.1	45.79	FE II	300	0.31	71		BL
2446.7	46.41	FE II	375	0.29	72		BL
2450.6	49.96	FE II	300		44	3.3	FE II BL
	50.20	FE II	300				
2451.7	51.21	FE II	209	0.49	44	2.4	
2454.3	53.75	FE II	375		45		BL
	53.94	FE II	375				BL
2455.0	54.57	FE II	320	0.53	63		BL
2457.4	57.10	FE II	269	0.30	28	2.4	
2459.2	58.78	FE II	209	0.42	74	4.5	
2462.1	61.28	FE II	209		77	5.7	
	61.86	FE II	209				
2464.0	63.28	FE II	208		56	5.3	
	63.73	FE II	162				
	64.01	FE II	208				
2465.4	64.90	FE II	208	0.50	67		
2467.2	66.67	FE II	179		66		
	66.81	FE II	179				
2469.9	69.51	FE II	299	0.39	59		
2472.9	72.43	FE II	179	0.47	40		BL+RM
2473.6	73.31	FE II	148	0.29	50		BL
2475.2	74.76	FE II	208	0.44			
2478.9	78.57	FE II	179	0.33	55	2.8	
2480.6	80.15	FE II	179	0.45	68	3.2	
2482.8	82.12	FE II	161		71	5.2	
	82.65	FE II	207				
2484.7	84.24	FE II	243		66	4.0	
	84.55	FE II	243				
2486.8	86.34	FE II	208	0.46	71	4.0	
2488.7	88.33	FE II	K	0.37	27	2.0	
2490.1	89.83	FE II	207	0.27	75		BL
2491.3	90.86	FE II	179		65		BL
	91.39	FE II	207				BL
2493.6	93.17	FE II	207		75	5.2	
	93.27	FE II	161				
2498.2	97.80	NI II	18		51		BL
	97.82	FE II	175				BL
	97.82	FE II	207				BL
2499.3	98.90	FE II	161	0.40	73		BL
2501.3	00.92	FE II	357	0.48	62	2.0	
2502.8	02.39	FE II	207	0.41	56		BL
2504.0	03.32	FE II	206		60	4.8	BL
	03.56	FE II	161				BL
	03.56	FE II	175				BL
	03.87	FE II	285				BL
2506.5	06.09	FE II	207		60	4.4	
	06.80	FE II	207				
2509.6	09.12	FE II	242	0.48	26	1.6	(?)
2511.8	10.87	NI II	18		73	6.8	
	11.76	FE II	161				
2515.9	14.38	FE II	285		58	4.4	
	14.91	FE II	206				
	14.91	FE II	175				
2517.7	17.21	FE II	207	0.49	46	3.6	RM
2519.5	19.04	FE II	268	0.46	64	3.2	
2521.6	21.09	FE II	268	0.51	63		BL
2522.3	21.81	FE II	330	0.49	54		BL
2523.3	22.89	FE II	K	0.41	61	3.2	
2526.2	25.11	FE II	330		79	8.0	BL

TABLE III *(continued)*.

OBS.WL	LAB.WL	ION	MULT	SHIFT	INT	FWHM	REMARKS
	25.39	FE II	159				BL
	26.07	FE II	159				BL
	26.29	FE II	145				BL
2527.7	27.11	FE II	159	0.59	51		BL
2529.9	29.08	FE II	357		69	4.7	
	29.22	FE II	241				
	29.54	FE II	145				
2534.1	33.63	FE II	159	0.47	78		BL
2534.8	34.41	FE II	159	0.39	70		BL
2535.9	35.48	FE II	177	0.42	55		
2537.2	36.67	FE II	241		75	3.9	
	36.82	FE II	159				
2539.2	38.79	FE II	158		71	5.5	
	38.90	FE II	158				
	39.00	FE II	158				
2541.3	40.67	FE II	177		70		BL
	41.10	FE II	177				BL
2542.3	41.83	FE II	158	0.47	59		BL
2543.8	43.38	FE II	159		70	4.7	
	43.43	FE II	177				
2545.6	45.22	FE II	159	0.38	68		BL
2547.1	46.67	FE II	177	0.43	60		BL
2550.2	48.59	FE II	158		63	11.4	RM
	49.40	FE II	177				
	49.45	FE II	177				
	50.02	FE II	240				
	50.56	FE II	158				
	50.68	FE II	240				
2555.6	55.07	FE II	177	0.53	46	2.7	
2557.9	57.50	FE II	175	0.40			
2560.5	59.24	FE II	266		59	5.1	
	59.92	FE II	267				
2563.0	62.54	FE II	64	0.46	83		BL,RM
2564.0	63.47	FE II	64	0.53	72		BL
2567.2	66.62	FE II	174		76	5.9	
	66.91	FE II	64				
2569.0	68.40	FE II	145		33	2.7	
	68.88	FE II	175				
2570.3	69.78	FE II	266	0.52	29	1.2	(?)
2571.3	70.84	FE II	284	0.46	58	2.4	
2574.8	74.36	FE II	144	0.44	71	2.7	
2576.8	76.11	MN II	1	0.69	86		BL
2578.4	77.92	FE II	64	0.48	72		BL
2583.1	82.58	FE II	64	0.52	84	3.5	
2586.4	85.88	FE II	1	0.52	100	4.6	
2588.4	88.95	FE II	326	0.45	55	2.7	
2592.1	91.54	FE II	64	0.56	77	3.8	BL
2593.3	92.78	FE II	318	0.52	69	3.5	BL
2594.1	93.72	FE II	64	0.38	57		BL
2594.4	93.73	MN II	1	0.67	82		BL
2598.8	98.37	FE II	1	0.43	88		BL
2599.9	99.39	FE II	1	0.53	100		BL
2605.7	05.42	FE II	204	0.28	57		BL
2606.3	05.70	MN II	1	0.60	83		BL
2607.4	07.09	FE II	1	0.31	83		BL
2612.3	11.87	FE II	1	0.43	86	5.4	
2614.3	13.82	FE II	1	0.48	87	3.8	
2618.1	17.62	FE II	1	0.48	84	4.2	
2619.6	19.07	FE II	171	0.53	32		
2621.0	20.41	FE II	1	0.59	60		BL
2622.2	21.67	FE II	1	0.53	72		BL
2624.2	23.72	FE II	171	0.48	20	3.1	
2626.0	25.66	FE II	1	0.34	83	4.2	
2626.9	26.50	FE II	173	0.40	30		
2628.7	28.29	FE II	1	0.41	77	3.8	
2630.3	29.59	FE II	171		54		BL
	30.07	FE II	171				BL
2631.7	31.04	FE II	1		87		BL
	31.32	FE II	1				BL
2654.2	53.57	CR II	8	0.63	25	3.4	
2659.0	58.59	CR II	8	0.41	30	4.9	
2665.0	64.66	FE II	263	0.34	72	4.5	BL CR II 8
2667.0	66.63	FE II	263	0.37	69	4.5	
2672.5	71.80	CR II	8	0.70	28	3.0	RM
2673.4	72.83	CR II	8	0.57	30	2.6	
2677.7	77.13	CR II	8		62	3.2	
	77.19	CR II	8				
2679.4	78.79	CR II	7	0.61	28	2.6	
2685.2	84.75	FE II	283	0.45	62	3.0	
2687.8	87.09	CR II	7	0.71	28	2.2	
2691.7	91.03	CR II	8	0.67	32	2.6	
2693.0	92.60	FE II	283		63	3.4	
	92.83	FE II	62				
2699.2	98.40	CR II	7		37		RM,(?)
	98.68	CR II	7				
2702.6							
2704.4	03.85	CR II	7		71	3.3	
	03.99	FE II	261				
2709.6	09.05	FE II	218		39	2.6	
	09.37	FE II	62				
2712.4	11.84	FE II	201		59	3.3	
	12.30	CR II	7				
2714.8	14.41	FE II	63	0.39	73	3.7	
2716.8	16.22	FE II	261		43	3.0	
	16.68	FE II	62				
2725.3	24.88	FE II	62	0.42			RM
2727.9	27.38	FE II	200		73	4.0	
	27.54	FE II	63				
2731.3	30.73	FE II	62	0.57	69	2.9	
2737.4	36.97	FE II	63	0.43	80	3.6	
2740.0	39.55	FE II	63	0.45	78	4.4	
2742.8	42.02	CR II	6	0.78	25		(?)
2743.7	43.20	FE II	62	0.50	74	3.6	
2747.1	46.49	FE II	62		80	5.8	FE II BL
	46.98	FE II	63				
2749.7	49.18	FE II	63		80	4.4	
	49.32	FE II	62				
	49.48	FE II	63				
2751.5	50.72	CR II	6		44	1.5	(?)
	50.90	FE II	200				
2752.6	51.85	CR II	6	0.75			RM
2753.7	53.29	FE II	235	0.41	75	3.3	
2756.2	55.73	FE II	62	0.47	77	4.0	
2758.4	57.72	CR II	6	0.68	28		
2762.3	61.81	FE II	63	0.49	54		BL
2763.4	62.58	CR II	6	0.72	44		BL
2765.0	64.79	FE II	198	0.21	15		
2767.9	66.55	CR II	6		66	5.1	
	67.50	FE II	235				
2769.7	68.94	FE II	63		52	2.9	
	69.15	FE II	200				
	69.35	FE II	198				
2779.7	79.30	FE II	234	0.40	59	2.9	
2784.1	83.69	FE II	234	0.41	68	3.6	
2791.3	90.77	MG II	3	0.52	35		
2794.5	93.89	FE II	198	0.61	41		BL
2796.2	95.52	MG II	1	0.68	100	7.1	BL
2798.7	97.99	MG II	3	0.71	30		BL
2799.6	99.29	FE II	233	0.31	18		BL
2803.3	02.69	MG II	1	0.61	100	5.4	BL MN I 1 ?
2823.2	22.67	FE II	231	0.53	31		
2829.2	28.62	FE II	231		30	2.9	
	28.68	FE II	255				
2832.0	30.94	FE II	280		61	4.6	
	31.56	FE II	217				
2836.3	35.63	CR II	5	0.67	68	3.0	
2839.7	39.53	FE II	391	0.17			
2841.0	40.64	FE II	217		47	3.5	
	40.76	FE II	280				
2843.9	43.24	CR II	5	0.66	50	2.8	
2848.5	48.12	FE II	399		19		
	48.33	FE II	391				
2850.5	49.83	CR II	5	0.67	49	3.2	
2852.9	52.12	MG I	1	0.68	81	1.8	
2856.3	55.67	CR II	5	0.63	49	3.2	
2857.7	56.93	FE II	399		24		BL
	57.17	FE II	294				BL
2858.8	58.34	FE II	279		45		BL
	58.52	FE II	354				BL
	58.64	FE II	399				BL
2859.7	58.91	CR II	5	0.79	43		BL
2861.6	60.92	CR II	5	0.68	33	2.6	
2863.2	62.57	CR II	5	0.63	43	2.8	
2865.7	65.10	CR II	5	0.60	39	2.8	
2867.3	66.72	CR II	5	0.58	41		
2868.3	67.65	CR II	5	0.65	27		
2874.0	73.40	FE II	279		34	3.2	
	73.46	CR II	5				
2875.9	75.34	FE II	258	0.56	16		BL
2876.9	76.24	CR II	5	0.66	35	2.8	BL
2878.9	77.97	CR II	5				
	78.45	CR II	5				
2881.3	80.75	FE II	61		41	2.8	
	80.83	FE II	258				
2884.3	83.71	FE II	230	0.59	32	3.1	
2890.4					24		
2895.5	94.78	FE II	230		25		
	95.21	FE II	294				
2927.0	26.58	FE II	60	0.42	40	2.0	
2929.4	28.62	MG II	2	0.78	21		(?)
2933.9	33.47	FE II	307	0.43	49	1.0	
2937.5	36.50	MG II	2	1.00	31		(?)
2940.0	39.51	FE II	60	0.49	47	2.4	
2945.0	44.40	FE II	78	0.60	46	2.6	
2948.2	47.66	FE II	78	0.54	49	2.7	
2949.9	49.18	FE II	277	0.72	53	2.1	(?)
2951.8	51.10	FE II	214	0.70			
2954.3	53.77	FE II	60	0.53	40	2.0	
2965.3	64.68	FE II	78				RM
	65.04	FE II	78				
2970.9	70.51	FE II	60	0.39	32		
2985.4	84.83	FE II	78	0.57	64	2.7	BL
2986.2	85.55	FE II	78	0.65	32		BL
3003.2	02.65	FE II	78	0.55	46	3.1	
3119.6	18.65	CR II	5	0.95	26	1.9	
3121.0	20.37	CR II	5	0.63	39	2.6	
3125.8	24.98	CR II	5	0.82	44	2.4	
3127.8					37	1.3	
3129.7	28.70	CR II	5	1.00			(?)
3132.9	32.06	CR II	5	0.84	43	3.2	

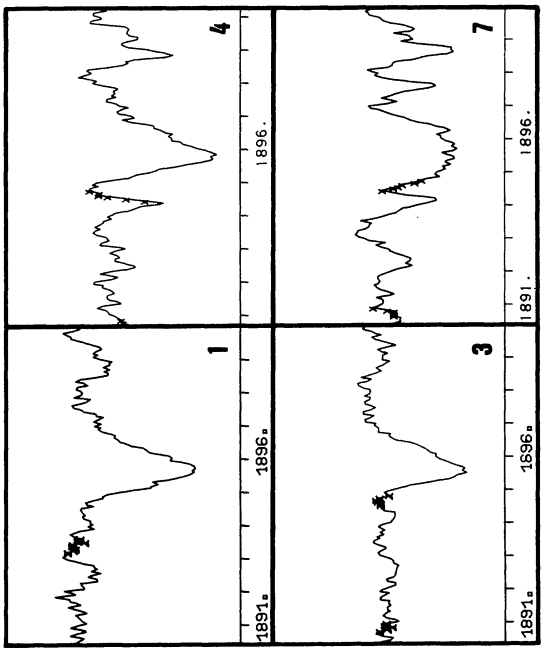

FIGURE 2. — One of the Fe III (34) lines, seen at different epochs.

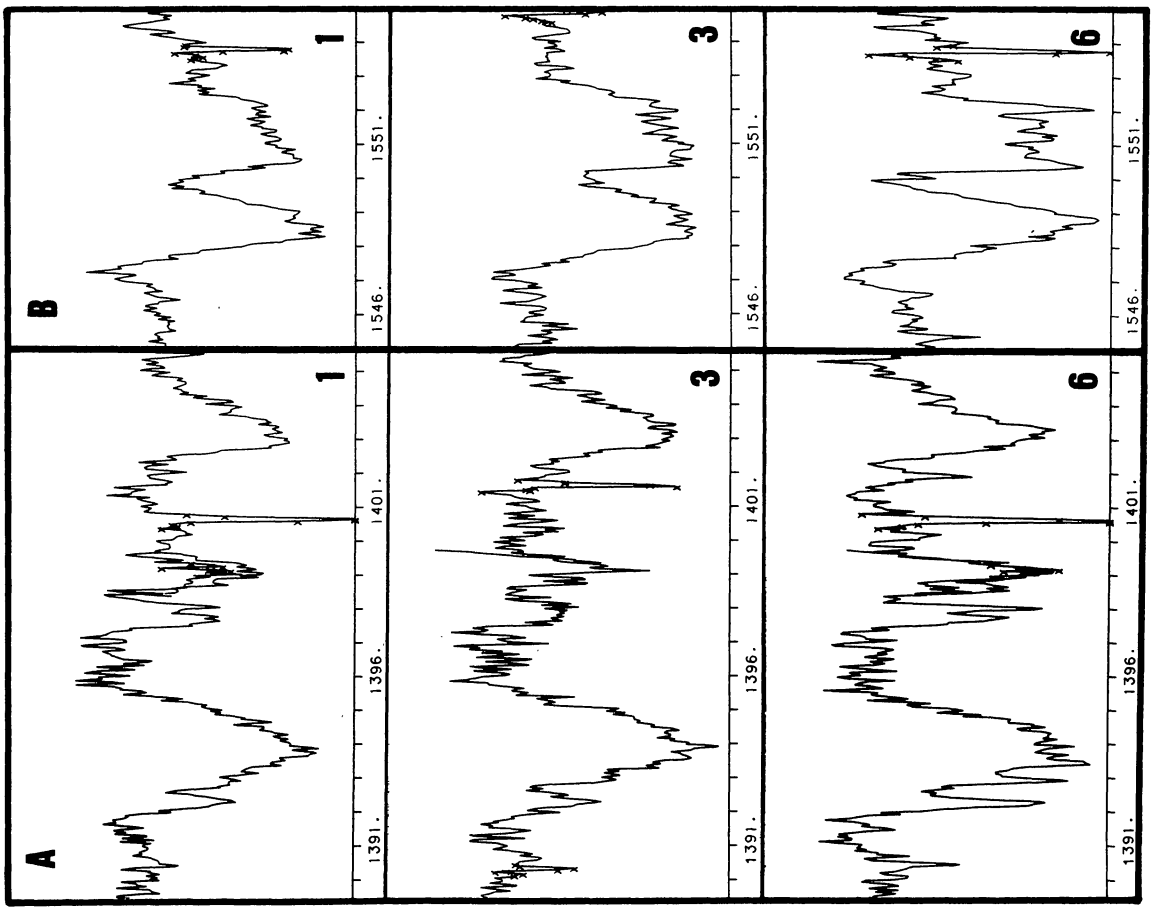

FIGURE 1. — The lines of the Si IV (A) and C IV (B) doublets, observed at different epochs. Some Fe II lines seem present (see text) : the lines at $\lambda\lambda$1392.15(K), 1392.82(K), 1393.21(K), 1404.12(K), 1401.77(K) are probably blended with the Si IV features while the lines at $\lambda\lambda$1548.69(46), 1550.26(45), 1551.93(K) seem to affect the C IV profile. The numbers refer to the spectra given in table I. The ordinates are relative intensities. The wavelength scale has not been corrected for earth's motion and is affected by the errors discussed in the text.

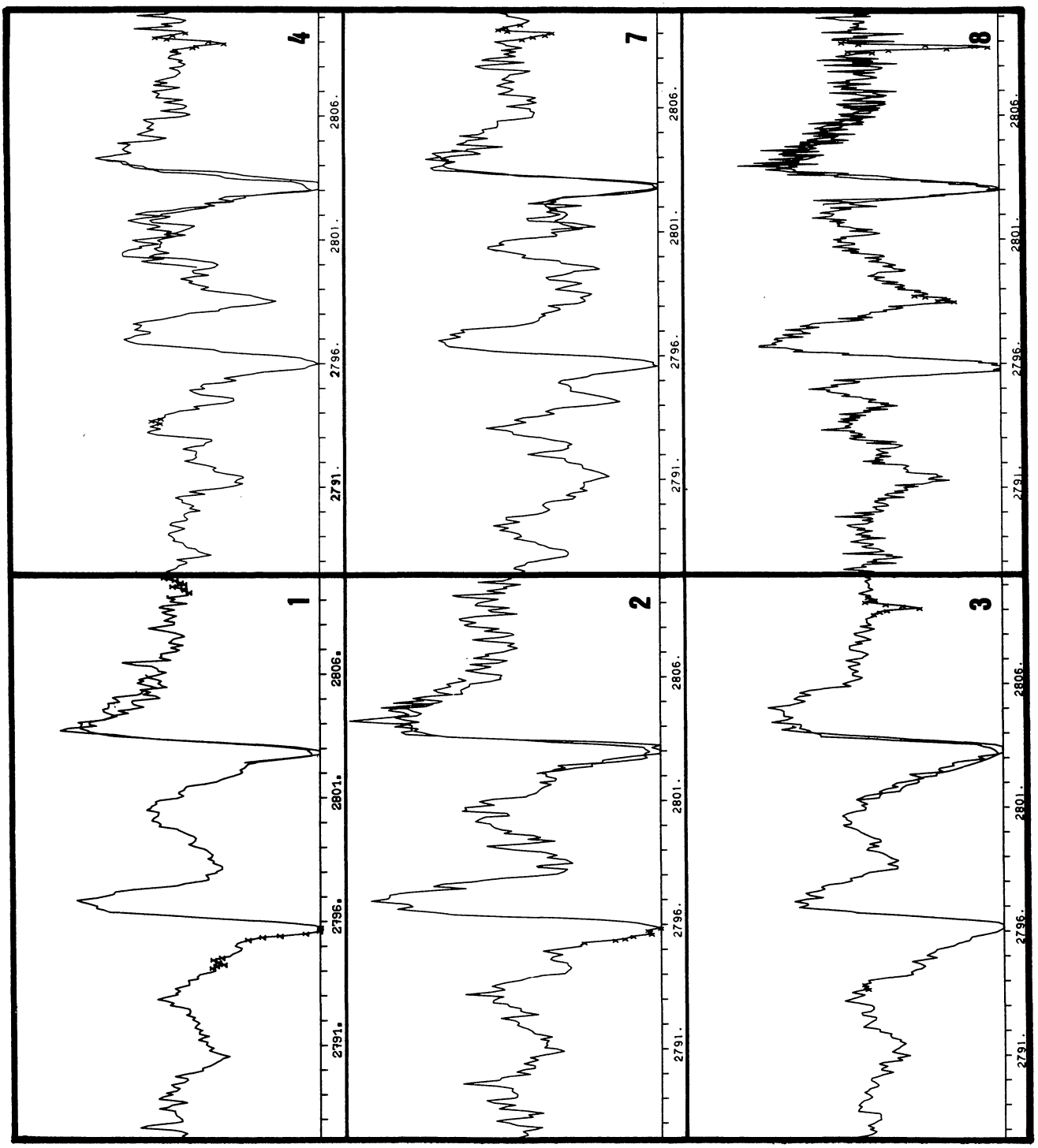

FIGURE 3. — Evolution of the Mg II doublet. Some features can be attributed to the Fe II lines at $\lambda\lambda$2792.05(233), 2793.89(198), 2799.29(233). Mn I is also suspected to be present.

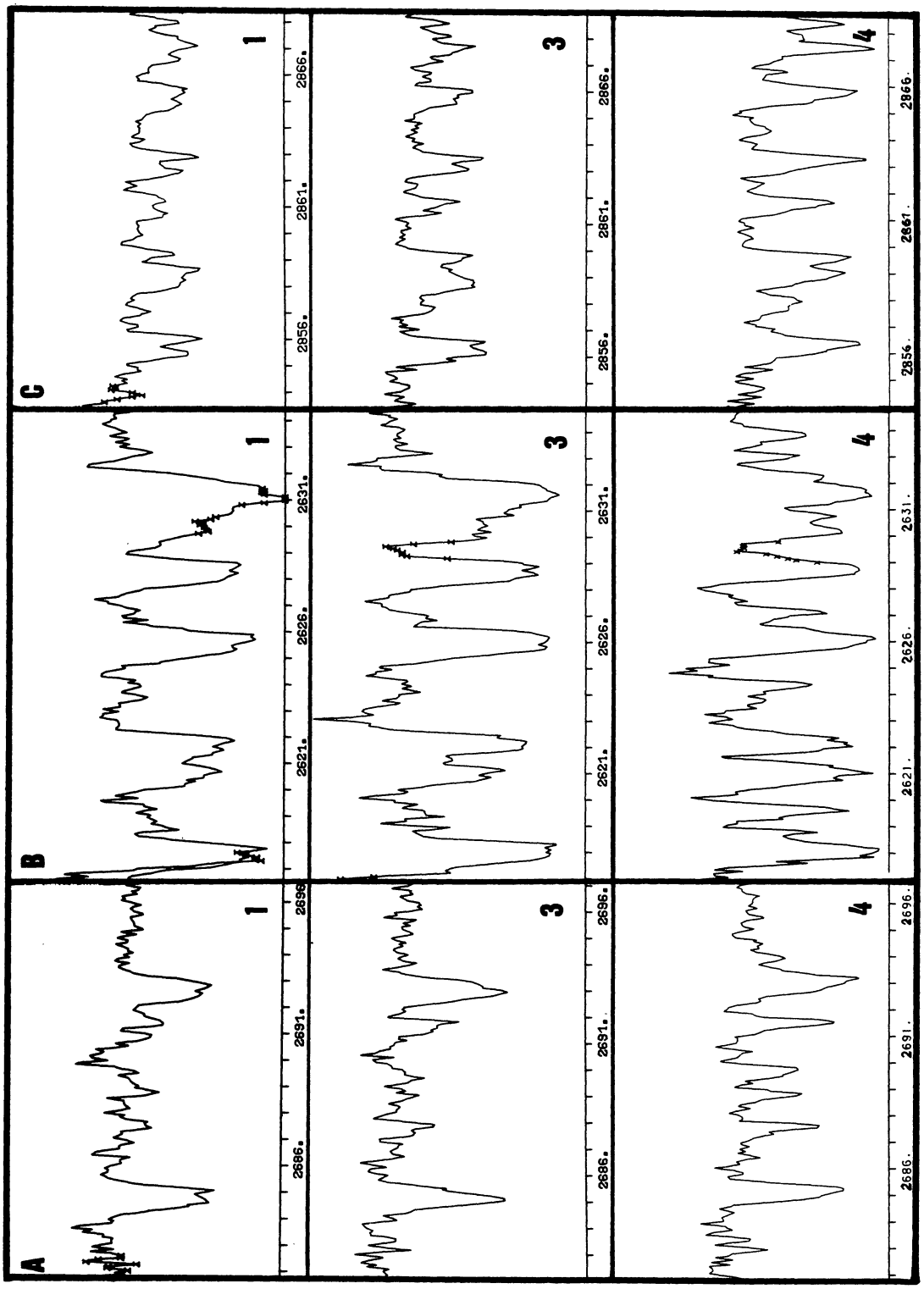

FIGURE 4. — The double structure of the absorption lines of the singly ionized elements observed in the regions of Fe II(283)-A-, Fe II(1)-B- and Cr II(5)-C-. Some features are clearly enhanced in the last spectrum and can be identified by -A- Cr II at λ2687.09, Fe II at λ2689.2(K) and -B- Fe II at $\lambda\lambda$2619.07(171), 2623.72(171), 2626.50(173), 2631.61(171).

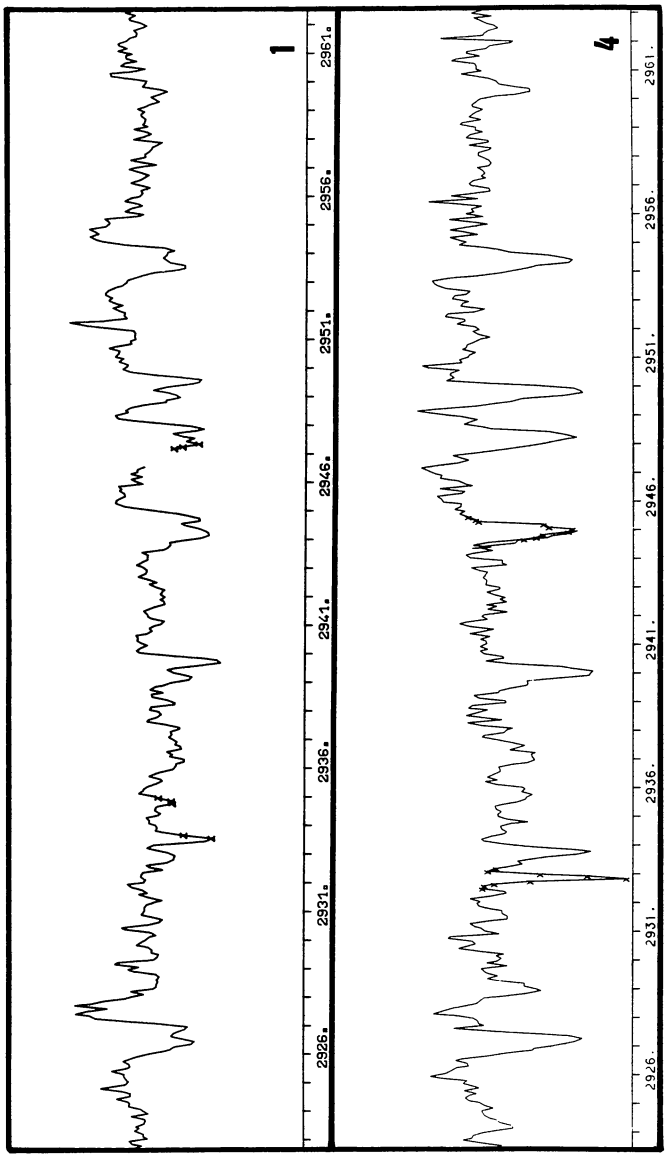

FIGURE 6. — The remarkable behavior of some Fe II lines (region of Fe II 60) between 1978 and 1980.

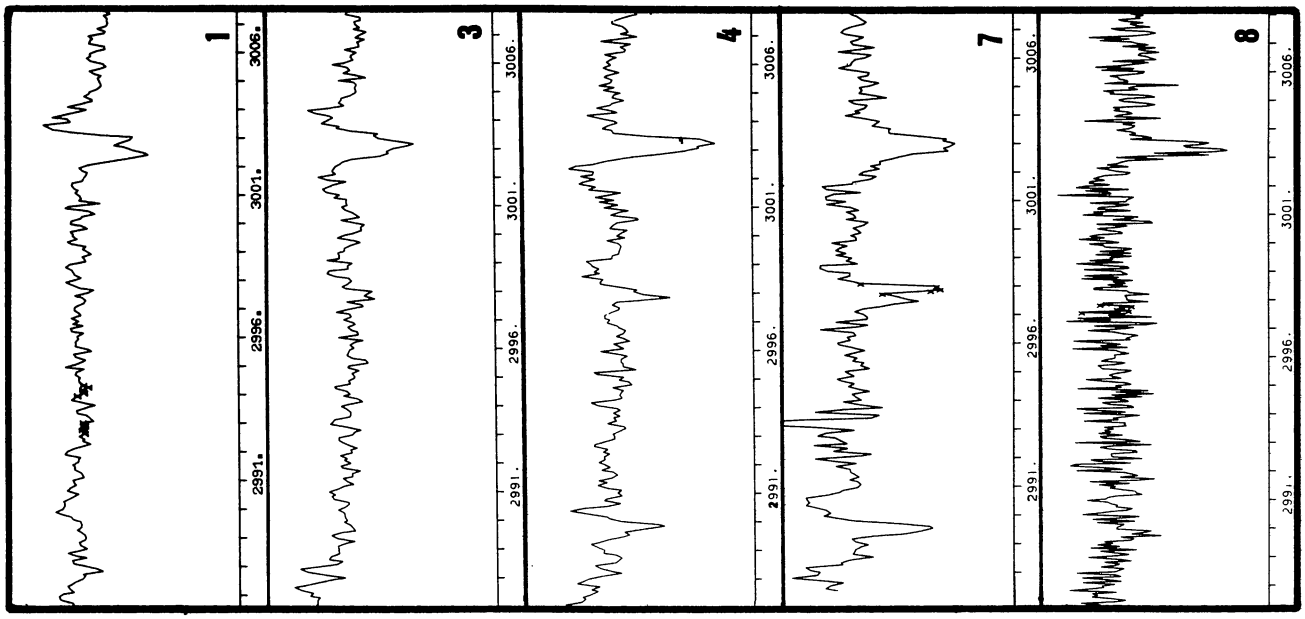

FIGURE 5. — The absorption/emission line variations in the Fe II (78) region with the enhancement of the Fe II lines at $\lambda\lambda$2989.37(291), 2989.73(291), 2997.30(335), 2997.75(292).

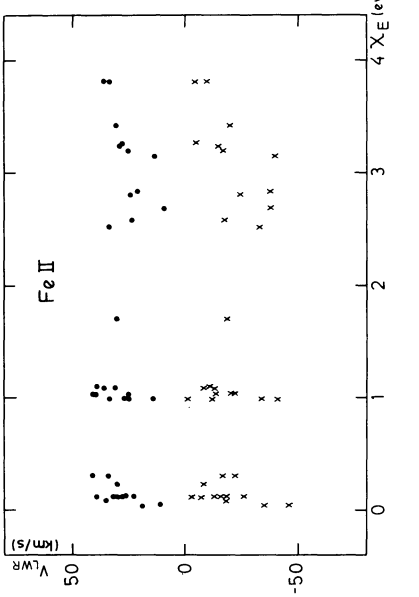

FIGURE 8. — The radial velocities of unblended Fe II absorption lines (LWR 3227) against the excitation potential of the lower level.

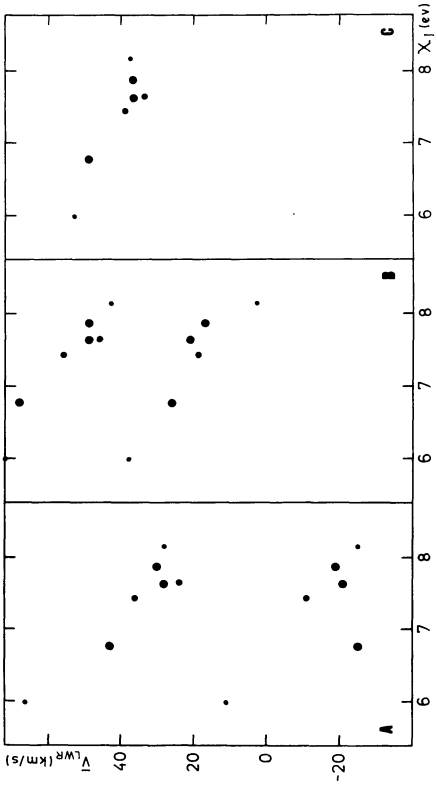

FIGURE 7. — The relation between the mean radial velocity of each component of the singly ionized element features and the ionization potential. Three epochs are represented : -A- DEC 1978, -B- MAR 1979 and -C- FEB 1980. The smaller the points, the less feasible are the measured velocities.

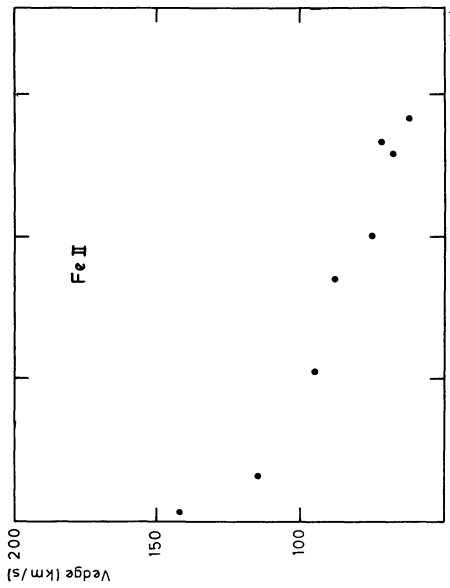

FIGURE 10. — The mean edge velocity ($\bar{\sigma} \sim 10$ km/s) of the Fe II absorption lines (measured in March 1979) against the excitation potential.

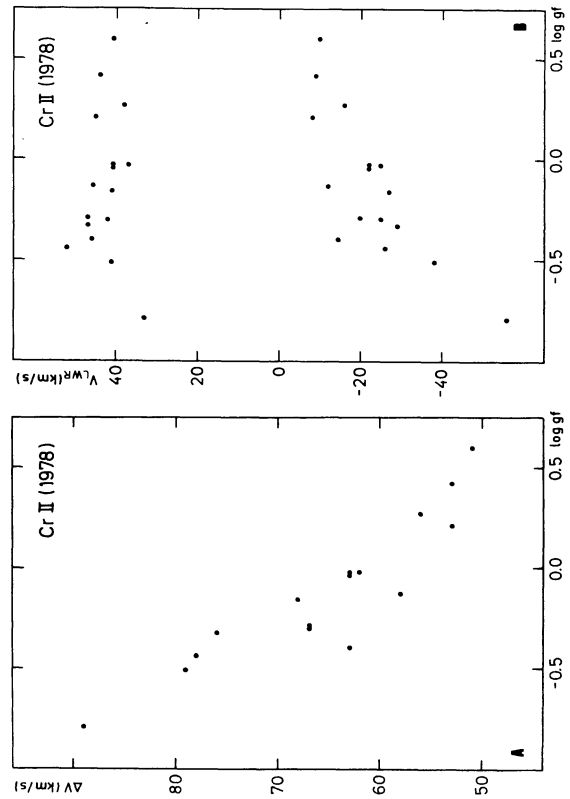

FIGURE 9. — The correlation between the radial velocities (measured in LWR 3227) of the Cr II absorption line components (B) or their difference (A) and the line strength.